

The Curvature Perturbation in the Axion-type Curvaton Model

Pravabati Chingangbam and Qing-Guo Huang

*School of physics, Korea Institute for Advanced Study,
207-43, Cheongryangri-2 Dong, Dongdaemun-Gu,
Seoul 130-722, Korea*

prava@kias.re.kr
huangqg@kias.re.kr

ABSTRACT

We study the axion-type curvaton model, with emphasis on the large field regime where analytic results are very difficult to obtain. We evaluate the tensor-scalar ratio r using WMAP normalization and the non-linearity parameters f_{NL} and g_{NL} by solving the equations numerically using the δN formalism. We compare them with results for the curvaton with quadratic potential. We find that r is much smaller for the axion-type case compared to the result from the quadratic potential, with the difference increasingly more pronounced at larger field values. g_{NL} is found to be positive, unlike the quadratic case where it is negative, and the amplitude of g_{NL} is much larger. Moreover, there is a nearly linear scaling between g_{NL} and f_{NL} , with small deviation from linearity at large field values. The slope between g_{NL} and f_{NL} depends on the parameters characterizing the axion-type curvaton model. We further consider a mixed scenario where both the inflaton and the curvaton contribute to the primordial power spectrum and the non-Gaussianity parameters are found to be much larger than those in the case with quadratic potential.

1 Introduction

Despite the simplicity of the inflationary paradigm [1], the mechanism by which curvature perturbations are generated is not yet fully established. An alternative to the standard scenario where the inflaton field is responsible for the accelerated expansion of the universe as well as the generation of curvature perturbations, is the curvaton mechanism [2]. This scenario has been gaining increasing popularity recently. According to this scenario the final perturbations are produced from initial isocurvature perturbation associated with quantum fluctuations of a light scalar field, the so-called curvaton, whose energy density is negligible during inflation. These curvaton isocurvature perturbations are transformed into adiabatic ones when the curvaton decays into radiation long after the end of inflation. It is also conceivable that the final curvature perturbations arise from a mixture of inflaton and curvaton perturbations. The curvaton scenario may naturally lead to much higher levels of local-type non-Gaussianity than standard single-field inflation.

The local-type non-Gaussianity can be characterized by some non-linearity parameters, namely, f_{NL} , g_{NL} and so on. They appear in the non-linear expansion of the curvature perturbation as:

$$\zeta(\mathbf{x}) = \zeta_g(\mathbf{x}) + \frac{3}{5}f_{NL}\zeta_g^2(\mathbf{x}) + \frac{9}{25}g_{NL}\zeta_g^3(\mathbf{x}) + \dots, \quad (1.1)$$

where ζ is the curvature perturbation in the uniform density slice, ζ_g denotes the Gaussian part of ζ . The primordial power spectrum, bispectrum and trispectrum are defined by

$$\langle \zeta(\mathbf{k}_1)\zeta(\mathbf{k}_2) \rangle = (2\pi)^3 \mathcal{P}_\zeta(k_1)\delta^3(\mathbf{k}_1 + \mathbf{k}_2), \quad (1.2)$$

$$\langle \zeta(\mathbf{k}_1)\zeta(\mathbf{k}_2)\zeta(\mathbf{k}_3) \rangle = (2\pi)^3 B_\zeta(k_1, k_2, k_3)\delta^3(\mathbf{k}_1 + \mathbf{k}_2 + \mathbf{k}_3), \quad (1.3)$$

$$\langle \zeta(\mathbf{k}_1)\zeta(\mathbf{k}_2)\zeta(\mathbf{k}_3)\zeta(\mathbf{k}_4) \rangle = (2\pi)^3 T_\zeta(k_1, k_2, k_3, k_4)\delta^3(\mathbf{k}_1 + \mathbf{k}_2 + \mathbf{k}_3 + \mathbf{k}_4). \quad (1.4)$$

The bispectrum and trispectrum are respectively related to the power spectrum by

$$B_\zeta(k_1, k_2, k_3) = \frac{6}{5}f_{NL}[\mathcal{P}_\zeta(k_1)\mathcal{P}_\zeta(k_2) + 2 \text{ perms}], \quad (1.5)$$

$$\begin{aligned} T_\zeta(k_1, k_2, k_3, k_4) &= \tau_{NL}[\mathcal{P}_\zeta(k_{13})\mathcal{P}_\zeta(k_3)\mathcal{P}_\zeta(k_4) + 11 \text{ perms}] \\ &\quad + \frac{54}{25}g_{NL}[\mathcal{P}_\zeta(k_2)\mathcal{P}_\zeta(k_3)\mathcal{P}_\zeta(k_4) + 3 \text{ perms}]. \end{aligned} \quad (1.6)$$

The parameter τ_{NL} depends on f_{NL} , as

$$\tau_{NL} = \frac{36}{25}f_{NL}^2, \quad (1.7)$$

if the total curvature perturbation is generated by only one field. The parameters f_{NL} , τ_{NL} and g_{NL} parameterize the non-Gaussianity from the irreducible three-point and four-point correlation functions respectively. See [3] for more discussions on the bispectrum and trispectrum.

In the simplest version of inflation model $f_{NL} \sim \mathcal{O}(n_s - 1)$ [4]. It is constrained by WMAP5 ($n_s = 0.96_{-0.013}^{+0.014}$) [5] to be much less than unity. Even though a Gaussian distribution of the primordial curvature perturbation is still consistent with WMAP5 ($-9 < f_{NL} < 111$, at 95% C.L.), the limit on f_{NL} on the negative side has been greatly reduced from WMAP3 to WMAP5, while still allowing for large positive value. The latest limit on this parameter is $f_{NL} = 38 \pm 21$ at 68% CL for the local shape non-Gaussianity in [6]. This has prompted many authors to consider different possible mechanisms for generating a large positive non-Gaussianity [7–13].

The curvaton is a light scalar field whose mass is small compared to the Hubble parameter H_* during inflation. It is sub-dominant during inflation and its fluctuations are initially of isocurvature type. After the end of inflation it is supposed to completely decay into thermalized radiation before primordial nucleosynthesis and the isocurvature perturbations generated by the curvaton are converted into final adiabatic perturbations. In order to prevent large quantum corrections to the curvaton mass and keep it small enough during inflation some symmetries are called for. It seems natural to invoke supersymmetry. However, supersymmetry must be broken above the inflation scale and the mass square of each scalar field generically receives a correction of order H_*^2 . So supersymmetry cannot be invoked to protect the smallness of curvaton mass.

A promising curvaton candidate is the pseudo-Nambu-Goldstone boson – axion [14], whose potential for the canonical field σ takes the form

$$V(\sigma) = m^2 f^2 \left(1 - \cos \frac{\sigma}{f}\right), \quad (1.8)$$

where f is called the axion decay constant. Actually the axion field is generic in various string models [15]. The smallness of the axion mass is protected by the shift symmetry $\sigma \rightarrow \sigma + \delta$. If $\sigma \ll f$, the curvaton potential is approximately quadratic, and the second order non-linearity parameter g_{NL} is expected to be small. However, g_{NL} is large if the non-quadratic term in the curvaton potential plays a significant role [9–11].

In the axion-type curvaton model, it is very hard to get analytic results if $\sigma \sim f$. This regime of large field value was studied numerically in [12] where the authors calculated f_{NL} . They concluded that it is quite similar to that of the quadratic potential if the curvaton accounts for the observed curvature perturbations. In this paper the curvature perturbation in the axion-type curvaton model will be studied in more detail, and we will see that the WMAP normalization and the second order non-linearity parameter g_{NL} are quite different from those of the quadratic one, in the large field regime. The curvature perturbation is calculated numerically using the δN formalism [16] and the results are compared with the quadratic model. We find that, as expected, r agrees

with the quadratic case at small field values. However, it is much smaller for larger field values and the difference increases rapidly as the field value increases. g_{NL} is positive and its amplitude is much larger than the quadratic case. We find that g_{NL} scales linearly with f_{NL} , with small deviation from linearity at large field values. The linear behavior is similar to the quadratic potential but the slope is quite different. We also analyze a mixed scenario where the primordial power spectrum has contributions from both the inflaton and the curvaton. We find that g_{NL} and f_{NL} are greatly suppressed with respect to the case where only the curvaton contributes. However, the suppression is much less for axion compared to the quadratic potential.

This paper is organized as follows: in Sec. 2, some analytic results for the curvaton model will be briefly reviewed. In Sec. 3, we numerically calculate the curvature perturbation for the axion-type curvaton model based on the δN formalism [16]. We calculate f_{NL} and g_{NL} and demonstrate the results in comparison to the quadratic potential and the potential with quartic correction. Next, we discuss the mixed scenario where the total primordial power spectrum has contributions from both the inflaton as well as the curvaton. Our results are summarized in Sec. 4. In an appendix we present a general discussion for the curvaton model with a small correction to the quadratic potential.

2 Analytic results for the curvaton model

We begin with a brief review of the curvaton model with quadratic potential. In the limit $\sigma \ll f$ the axion-type curvaton potential is reduced to this case. The amplitude of the primordial power spectrum generated by the curvaton with quadratic potential

$$V(\sigma) = \frac{1}{2}m^2\sigma^2 \quad (2.1)$$

is given by

$$P_{\zeta_\sigma} = \frac{1}{9\pi^2}f_D^2\frac{H_*^2}{\sigma_*^2}, \quad (2.2)$$

where H_* and σ_* are the Hubble parameter and the vacuum expectation value of curvaton field evaluated at Hubble exit during inflation, respectively, and

$$f_D = \frac{3\Omega_{\sigma,D}}{4 - \Omega_{\sigma,D}}, \quad \Omega_{\sigma,D} = \frac{\rho_\sigma}{\rho_{tot}} \quad (2.3)$$

evaluated at the time of curvaton decay. WMAP normalization [5] requires

$$P_{\zeta,obs} = 2.457_{-0.093}^{+0.092} \times 10^{-9}. \quad (2.4)$$

The amplitude of the tensor perturbation only depends on the scale of inflation, as,

$$P_T = \frac{H_*^2/M_p^2}{\pi^2/2}. \quad (2.5)$$

The tensor-scalar ratio is defined as $r \equiv P_T/P_\zeta$ and then the WMAP normalization ($P_\zeta = P_{\zeta,obs}$) implies that the Hubble scale during inflation is related to r by

$$H_* \simeq 1.1 \times 10^{-4} r^{\frac{1}{2}} M_p. \quad (2.6)$$

Usually the dimensionless parameter r is used to characterize the inflation scale H_* . If the total amplitude of the primordial power spectrum is generated by the curvaton, namely $P_{\zeta_\sigma} = P_{\zeta,obs}$, then r is given by

$$r = \frac{18}{f_D^2} \frac{\sigma_*^2}{M_p^2}, \quad (2.7)$$

which encodes the WMAP normalization. Since the potential takes the quadratic form, the curvaton field evolves linearly after inflation and the non-Gaussianity parameters f_{NL} and g_{NL} are respectively given by [17],

$$f_{NL} = \frac{5}{4f_D} - \frac{5}{3} - \frac{5f_D}{6}, \quad (2.8)$$

$$g_{NL} = \frac{25}{54} \left(-\frac{9}{f_D} + \frac{1}{2} + 10f_D + 3f_D^2 \right). \quad (2.9)$$

For large positive f_{NL} , $f_D \ll 1$, which implies

$$g_{NL} \simeq -\frac{10}{3} f_{NL}. \quad (2.10)$$

Since g_{NL} is the coefficient of ζ_g^3 , it is very difficult to measure g_{NL} in the near future if it is the same order of f_{NL} .

After inflation the universe is dominated by radiation and hence the Hubble parameter goes like a^{-2} . Roughly, the curvaton does not evolve until $H = m$. Once the Hubble parameter drops below the curvaton mass, the curvaton field rolls down its potential and starts to oscillate around its minimum. The energy density of an oscillating curvaton field with quadratic potential goes like dust-like matter ($\sim a^{-3}$) and grows with respect to that of radiation. When the Hubble parameter is roughly the same as the curvaton decay rate Γ_σ , the curvaton starts to decay into radiation. For simplicity, the curvaton is assumed to suddenly decay into radiation at the time of $H = \Gamma_\sigma$. Let us assume the scale factor equals to 1 at the time of $H = m$, and the scale factor is denoted by a when $H = \Gamma_\sigma$. If $\sigma_* \ll M_p$, the radiation and curvaton energy densities are respectively $3M_p^2 m^2$ and $\frac{1}{2} m^2 \sigma_*^2$ at the time of $H = m$, and thus,

$$3M_p^2 m^2 a^{-4} + \frac{1}{2} m^2 \sigma_*^2 a^{-3} = 3M_p^2 \Gamma_\sigma^2. \quad (2.11)$$

The curvaton energy density parameter at the time of its decay can be written by

$$\Omega_{\sigma,D} = \frac{m^2 \sigma_*^2}{6M_p^2 \Gamma_\sigma^2} a^{-3}. \quad (2.12)$$

If $\frac{\Gamma_\sigma}{m} \ll \frac{\sigma_*^4}{M_p^4}$, then, $a \simeq (\frac{m^2 \sigma_*^2}{6M_p^2 \Gamma_\sigma^2})^{1/3}$ and $\Omega_{\sigma,D} \simeq 1$, which gives, $f_{NL} \simeq -5/6$. If, on the other hand, $\frac{\Gamma_\sigma}{m} \gg \frac{\sigma_*^4}{M_p^4}$, then, $a = \sqrt{m/\Gamma_\sigma}$, and

$$\Omega_{\sigma,D} \simeq \frac{\sigma_*^2}{6M_p^2} \sqrt{\frac{m}{\Gamma_\sigma}}. \quad (2.13)$$

This gives

$$f_D \simeq \frac{3}{4} \Omega_{\sigma,D} \simeq \frac{\sigma_*^2}{8M_p^2} \sqrt{\frac{m}{\Gamma_\sigma}}, \quad (2.14)$$

which is much smaller than 1, and hence we get $f_{NL} \simeq \frac{5}{4f_D} \gg 1$. In this paper we focus on the latter case with large positive f_{NL} . Combining Eqs.(2.7) and (2.14) we get

$$r = 1152 \frac{\Gamma_\sigma}{m} \frac{M_p^2}{\sigma_*^2}. \quad (2.15)$$

f_{NL} and g_{NL} are respectively given by

$$f_{NL} \simeq 10 \sqrt{\frac{\Gamma_\sigma}{m}} \frac{M_p^2}{\sigma_*^2}, \quad (2.16)$$

$$g_{NL} \simeq -\frac{100}{3} \sqrt{\frac{\Gamma_\sigma}{m}} \frac{M_p^2}{\sigma_*^2}. \quad (2.17)$$

We see that WMAP normalization implies

$$\frac{\Gamma_\sigma}{m} \simeq 10^{-4} \left(\frac{r}{f_{NL}} \right)^2. \quad (2.18)$$

Then, if $r \sim 10^{-2}$ and $f_{NL} \sim 10^2$, $\Gamma_\sigma/m \sim 10^{-12}$.

In order to compare with the results of the axion-type curvaton model, it is better to re-scale the curvaton field to be $\theta \equiv \sigma/f$, and we get

$$f_D \simeq \frac{\theta_*^2}{8} \frac{f^2}{M_p^2} \sqrt{\frac{m}{\Gamma_\sigma}}, \quad (2.19)$$

$$r = \frac{18}{f_D^2} \frac{f^2}{M_p^2} \theta_*^2. \quad (2.20)$$

In this paper, we choose $f/M_p = 5 \times 10^{-3}$ and $\Gamma_\sigma/m = 10^{-4}$ which are the same as those in [12]. This gives, $f_D = 3.125 \times 10^{-4} \theta_*^2$, and $r = 4.6 \times 10^3 \theta_*^{-2}$. For $\theta_* \ll 1$, we get $r \gtrsim 10^3$, which is not compatible with the bound from WMAP5 of $r < 0.20$.

On the other hand, if r is required to satisfy the bound from WMAP5, the curvature perturbation generated by curvaton will be much smaller than $P_{\zeta,obs}$ for $\theta_* \ll 1$. We will more carefully discuss this case in Sec. 3.2. If we tune Γ_σ/m to be very small, for example 10^{-12} , $r < 0.2$ and $P_{\zeta_\sigma} = P_{\zeta,obs}$ can be achieved. But numerical calculation becomes much more difficult as we decrease Γ_σ/m and is not much more instructive. So, in this paper, we keep $f/M_p = 5 \times 10^{-3}$ and $\Gamma_\sigma/m = 10^{-4}$ fixed and illustrate the physics.

In [10], the cosine-type potential of curvaton is expanded to the second order,

$$V \simeq \frac{1}{2}m^2 f^2 \theta^2 \left(1 - \frac{1}{12}\theta^2 + \dots \right), \quad (2.21)$$

and the second term in the bracket is taken as a correction for small θ values. Taking into account the non-linear evolution of curvaton after inflation but prior to oscillation, the non-linearity parameters are given by

$$f_{NL} = \frac{5}{4f_D}(1 + h_2) - \frac{5}{3} - \frac{5f_D}{6}, \quad (2.22)$$

$$g_{NL} = \frac{25}{54} \left(\frac{9}{4f_D^2}(h_3 + 3h_2) - \frac{9}{f_D}(1 + h_2) + \frac{1}{2}(1 - 9h_2) + 10f_D + 3f_D^2 \right). \quad (2.23)$$

where

$$h_2 = \frac{1.135\delta(0.951 + 0.189\delta)}{(0.951 + 0.568\delta)^2}, \quad (2.24)$$

$$h_3 = \frac{1.135\delta(0.951 + 0.189\delta)^2}{(0.951 + 0.568\delta)^3}, \quad (2.25)$$

$$\delta = \frac{\theta_*^2}{24}. \quad (2.26)$$

If $\theta_* \ll 1$, the above results are the same as those of quadratic potential. Since h_2 is positive, f_{NL} is enhanced due to the correction. Another important feature is that g_{NL} is expected to be large and positive for large θ_* . Even though this expansion is not reliable for large values of θ (see Fig. 1), (note, in particular, that the potential $\theta^2/2 - \theta^4/24$ approaches its maximum value at around $\theta = \pm 0.78\pi$), we will naively use the above formula to calculate f_{NL} and g_{NL} , and compare them to the numerical results in Sec. 3.1.

Before we end this section, we would like to mention the vacuum expectation value (VEV) of the curvaton during inflation. At the classical level, the VEV of the curvaton is taken as a free parameter. However, in a long-lived inflationary universe, the long wavelength modes of the quantum fluctuation of a light scalar field may play a crucial role in its behavior, because its Compton wavelength is large compared to the Hubble size during inflation. In [18], the vacuum expectation value of the square of such a light

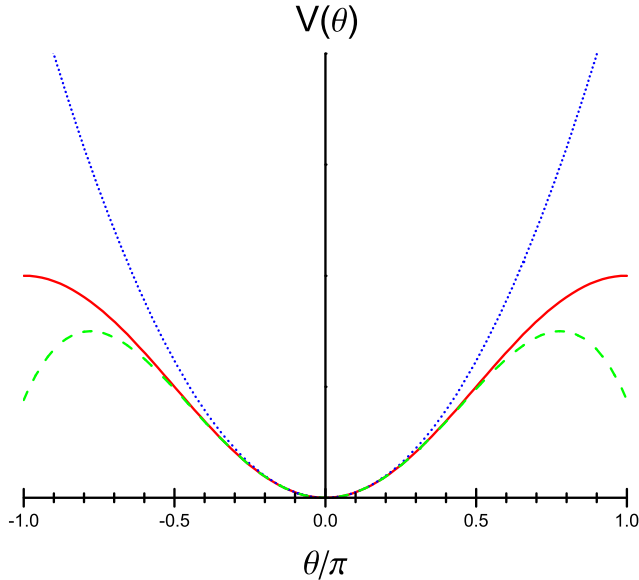


Figure 1: The red (solid), blue (dotted) and green (dashed) lines correspond to the axion potential, quadratic potential and $\theta^2/2 - \theta^4/24$ respectively.

scalar field with potential $V(\sigma) = \frac{1}{2}m^2\sigma^2$ is given by

$$\langle\sigma^2\rangle = \frac{3H_*^4}{8\pi^2 m^2}, \quad (2.27)$$

where H_* is the Hubble parameter during inflation. Typically the vacuum expectation value of σ can be estimated as

$$\sigma_* = \sqrt{\langle\sigma^2\rangle} = \sqrt{\frac{3}{8\pi^2} \frac{H_*^2}{m}}. \quad (2.28)$$

For a curvaton field with quadratic potential, its typical vacuum expectation value is given by H_*^2/m and its energy density is roughly H_*^4 . Larger the Hubble parameter during inflation, larger the energy density of curvaton. However, the energy density of axion-type curvaton is bounded by $m^2 f^2$ from above. If $mf \gg H_*^2$, σ_* can be estimated as H_*^2/m . On the other hand, $\sigma_* \sim f$ if $mf \leq H_*^2$. Since it is difficult to get analytic results for the axion-type curvaton model if $\sigma_* \sim f$, we will use numerical method to calculate the curvature perturbation in the next section.

3 Numerical results of the curvature perturbation

The curvature perturbation on sufficiently large scales on the uniform density slicing can be computed by the δN formalism [16]. Starting from any initial flat slice at time t_{ini} , on the uniform density slicing, the curvature perturbation is given by

$$\zeta(t, \mathbf{x}) = \delta N = N(t, \mathbf{x}) - N_0(t), \quad (3.1)$$

where $N(t, \mathbf{x}) = \ln(a(t, \mathbf{x})/a(t_{ini}))$, and $N_0(t) = \ln(a(t)/a(t_{ini}))$ is the unperturbed amount of expansion. In the following subsections we will study two different curvaton scenarios, first, the curvature perturbation is generated by the curvaton alone, and secondly, the curvature perturbation is a mixture of inflaton and curvaton perturbations.

3.1 Primordial power spectrum mainly generated by curvaton

In this subsection we focus on the curvaton model in which the curvature perturbation is generated by a curvaton field. The curvature perturbation can be expanded as

$$\zeta = N_{,\sigma}\delta\sigma + \frac{1}{2}N_{,\sigma\sigma}\delta\sigma^2 + \frac{1}{6}N_{,\sigma\sigma\sigma}(\delta\sigma)^3 + \dots \quad (3.2)$$

where $N_{,\sigma} = dN/d\sigma$, $N_{,\sigma\sigma} = d^2N/d\sigma^2$ and so on. Since $\delta\sigma = \frac{H_*}{2\pi}$, the amplitude of the curvature perturbation generated by curvaton takes the form

$$P_{\zeta\sigma} = N_{,\sigma}^2 \left(\frac{H_*}{2\pi} \right)^2, \quad (3.3)$$

and the non-Gaussianity parameters are given by

$$f_{NL} = \frac{5}{6} \frac{N_{,\sigma\sigma}}{N_{,\sigma}^2}, \quad g_{NL} = \frac{25}{54} \frac{N_{,\sigma\sigma\sigma}}{N_{,\sigma}^3}. \quad (3.4)$$

After inflation, the vacuum energy which governs the dynamics of the inflaton is converted to radiation and the equations of motion of the universe are

$$H^2 = \frac{1}{3M_p^2}(\rho_r + \rho_\sigma), \quad (3.5)$$

$$\dot{\rho}_r + 4H\rho_r = 0, \quad (3.6)$$

$$\rho_\sigma = \frac{1}{2}\dot{\sigma}^2 + V(\sigma), \quad (3.7)$$

$$\ddot{\sigma} + 3H\dot{\sigma} + \frac{dV(\sigma)}{d\sigma} = 0, \quad (3.8)$$

where ρ_r and ρ_σ are the energy densities of radiation and curvaton. It is convenient to define new dimensionless quantities, namely $N(t) = \ln a(t)$, $x = mt$ and $\theta = \sigma/f$. Then

the above equations of motion are simplified to be

$$\frac{dN}{dx} = \left[\alpha e^{-4N} + \frac{f^2}{3M_p^2} \left(\frac{1}{2} \left(\frac{d\theta}{dx} \right)^2 + \tilde{V}(\theta) \right) \right]^{\frac{1}{2}}, \quad (3.9)$$

$$\frac{d^2\theta}{dx^2} + 3 \frac{dN}{dx} \frac{d\theta}{dx} + \frac{d\tilde{V}(\theta)}{d\theta} = 0, \quad (3.10)$$

where

$$V(\sigma) = m^2 f^2 \tilde{V}(\theta), \quad (3.11)$$

and

$$\alpha = \frac{\rho_{r,ini}}{3M_p^2 m^2}, \quad (3.12)$$

and $\rho_{r,ini}$ is the radiation energy density at $t = t_{ini}$. For the axion-type curvaton model, $\tilde{V}(\theta) = 1 - \cos\theta$. The scale factor can be rescaled to satisfy $a(t_{ini}) = 1$ and then $N(t_{ini}) = 0$. Roughly speaking, the number of e-folds from the end of inflation to the beginning of the curvaton oscillations is almost unperturbed and the time when $H = m \frac{dN}{dx} = m$ can be taken as the initial time t_{ini} for simplicity. Because the energy density of radiation is still much larger than that of curvaton when $H = m$, $\rho_{r,ini} = 3M_p^2 m^2$ and then $\alpha = 1$. Here we adopt the curvaton sudden-decay approximation which says that the curvaton is proposed to suddenly decay into radiation at the time of $H = \Gamma_\sigma$. This condition is used to stop the evolution of curvaton in the numerical calculation. We must mention that all our numerical results presented in the following are for $f = 5 \times 10^{-3} M_p$ and $\Gamma_\sigma/m = 10^{-4}$, unless otherwise specified.

First of all, we want to compare the analytic results for the curvaton model with quadratic potential to the numerical results. In this case, the non-Gaussianity parameters only depend on the parameter f_D . We numerically calculate exact f_D which is given in Eq. (2.3) and show it along with the analytic approximate expression for f_D given in Eq. (2.19) in Fig. 2. We see that the exact numerical result (blue dashed line) is larger than the analytic approximation (black dotted line) by about factor of two. The reason is that the energy density of the curvaton, as it oscillates about its minimum potential, does not exactly decrease as fast as a^{-3} , due to the friction term $3H\dot{\sigma}$, even though this term is small compared to the driving term $m^2\sigma$. So the curvaton energy density at the time of its decay is slightly larger than the analytic approximation.

Using the dimensionless quantities used in the numerical calculation, the amplitude of the power spectrum of the curvature perturbation generated by the curvaton is denoted by

$$P_{\zeta_\sigma} = N_*'^2 \frac{H_*^2}{4\pi^2 f^2}, \quad (3.13)$$

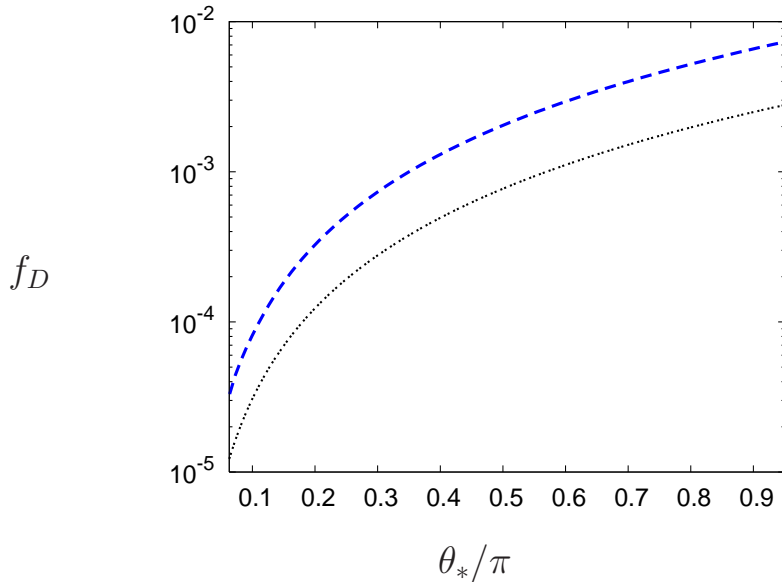


Figure 2: The blue (dashed) line shows the exact value of f_D computed numerically, whereas, the black (dotted) line shows to f_D computed from the analytic approximation in Eq.(2.19), for the quadratic potential.

where

$$N'_* = \left. \frac{dN_{tot}}{d\theta_{ini}} \right|_{\theta_{ini}=\theta_*}, \quad (3.14)$$

and N_{tot} denotes the total number of e-folds from t_{ini} to the time of $H = \Gamma_\sigma$. The tensor-scalar ratio r (or the inflation scale H_*) is determined by WMAP normalization as

$$r = \frac{8}{N_*'^2} \frac{f^2}{M_p^2}. \quad (3.15)$$

The numerical result for r is shown in Fig. 3 where we have plotted for axion-type (red solid lines) and quadratic case (blue dotted lines). The upper set of red and blue lines correspond to $\Gamma_\sigma/m = 10^{-4}$, while the lower set corresponds to $\Gamma_\sigma/m = 10^{-5}$. From this figure we see agreement of the value of r between the two models for $\theta_* \ll 1$. As θ_* increases we find that r for the axion-type potential increasingly becomes smaller than the quadratic potential. r seems to scale linearly with Γ_σ/m for the axion-type model, as is the case for the quadratic potential, as seen in Eq. (2.15). Hence, for large field values it is possible to satisfy WMAP normalization and the constraint on r simultaneously for much larger values of Γ_σ/m , as compared to the quadratic case.

The non-linearity parameters are given by

$$f_{NL} = \frac{5}{6} \frac{N_*''}{N_*'^2}, \quad g_{NL} = \frac{25}{54} \frac{N_*'''}{N_*'^3}, \quad (3.16)$$

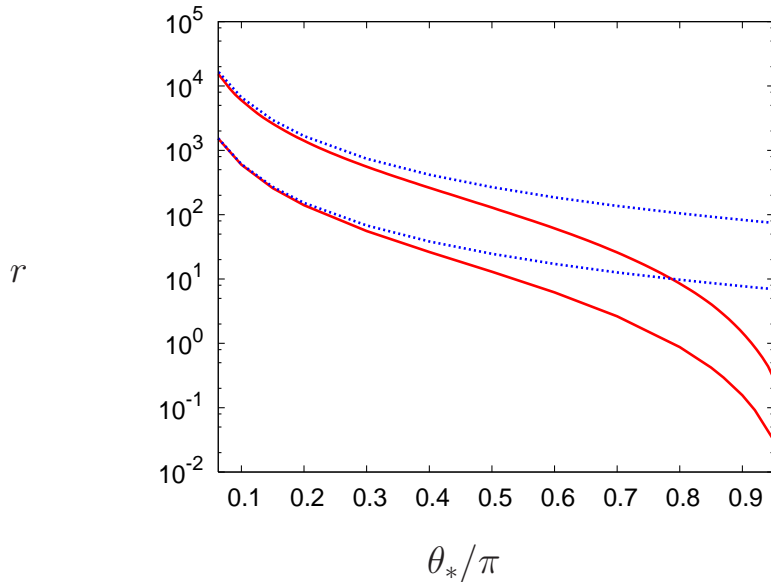


Figure 3: The red (solid) line shows r for the cosine potential and the blue (dotted) line for the quadratic potential, respectively, for $\Gamma_\sigma/m = 10^{-4}$ and 10^{-5} . r is seen to decrease as Γ_σ/m decreases.

where

$$N_*'' = \left. \frac{d^2 N_{tot}}{d\theta_{ini}^2} \right|_{\theta_{ini}=\theta_*}, \quad \text{and} \quad N_*''' = \left. \frac{d^3 N_{tot}}{d\theta_{ini}^3} \right|_{\theta_{ini}=\theta_*}, \quad (3.17)$$

Fig. 4 shows the numerical results of f_{NL} for axion-type (red solid line), quadratic (blue dotted line), and quadratic with correction (green dashed line) models. We see that the three results agree very well for small θ_* and begins to differ as θ_* increases. The difference, however, is only of order one and hence small. Fig. 4 gives a confirmation of the results of [12]. The correction case is not really correct at large θ_* but we still plot it to show the agreement at small θ_* .

Next we look at the results for g_{NL} for the same three models as above. The numerical results are plotted in Fig. 5. The red solid line shows the result for the axion-type curvaton, and we can see that g_{NL} is positive and larger than the magnitudes for the other two cases. For the quadratic case, we know from the analytic expression of Eq. (2.9) that it is negative and that is shown by the blue dotted line which gives the exact numerical answer. Again we know from Eq. (2.23) that for correction case it is positive and that is what we see from the green dashed line in the figure.

From Fig. 6 where we have plotted g_{NL} versus f_{NL} an interesting observation is that g_{NL} almost linearly depends on f_{NL} for the axion-type curvaton model, namely

$$g_{NL} \simeq c f_{NL}, \quad (3.18)$$

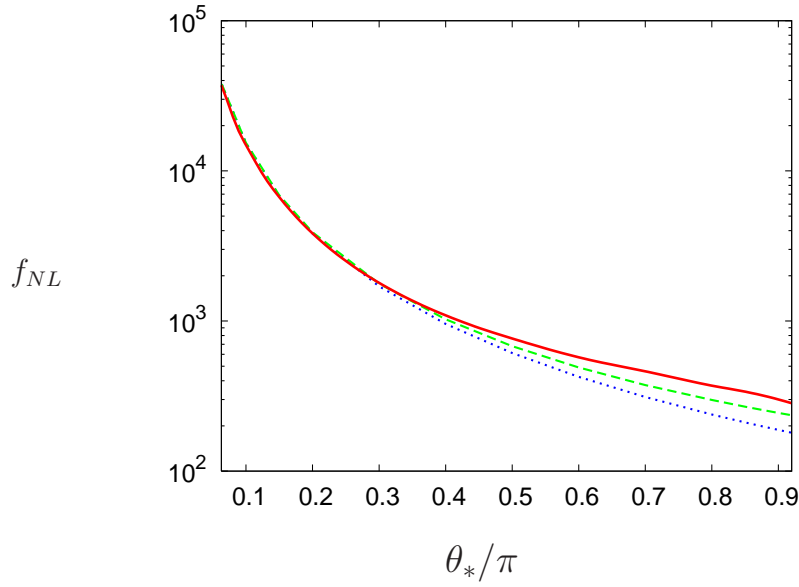


Figure 4: Plot of f_{NL} . The red (solid), blue (dotted) and green (dashed) lines correspond to axion-type, quadratic and quadratic with σ^4 correction models, respectively.

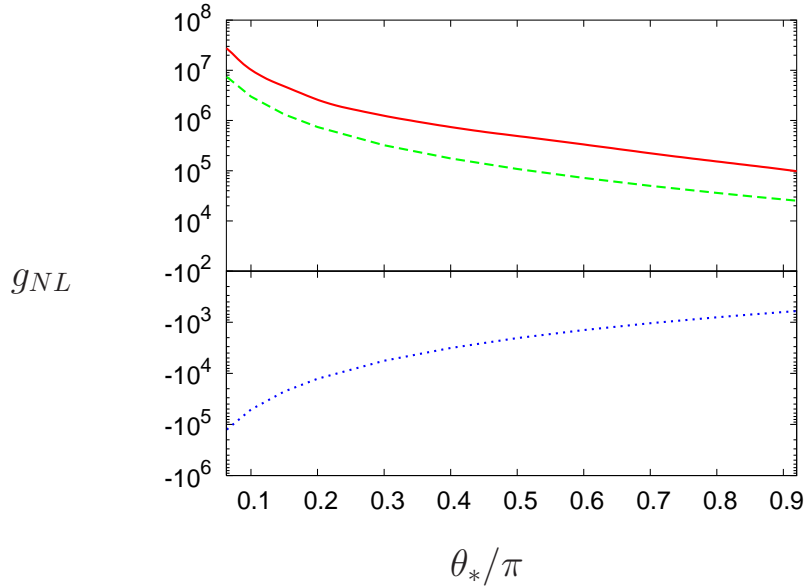


Figure 5: Plot of g_{NL} . The red (solid), blue (dotted) and green (dashed) lines correspond to axion-type, quadratic and quadratic with σ^4 correction models, respectively.

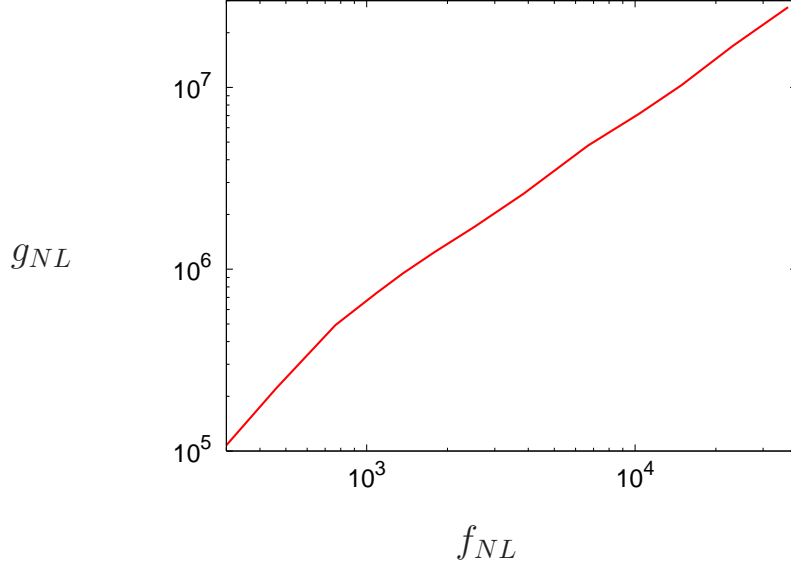


Figure 6: Plot of g_{NL} vs. f_{NL} for axion-type curvaton.

where $c \simeq 732$. From Fig. 4 and 5, we can see that the formulas for the quadratic with correction capture some features of the axion-type curvaton model. Here we try to use them to roughly understand why g_{NL} almost linearly depends on f_{NL} . At the leading order, we have

$$h_2 \simeq h_3 \simeq 1.193\delta = 0.05\theta_*^2, \quad (3.19)$$

and then

$$f_{NL} \simeq 1.25/f_D, \quad g_{NL} \simeq 0.21\theta_*^2/f_D^2. \quad (3.20)$$

Taking into account the analytic formula for f_D in Eq. (2.19), we obtain

$$f_{NL} \simeq 10 \frac{M_p^2}{f^2} \sqrt{\frac{\Gamma_\sigma}{m}} \theta_*^{-2}, \quad (3.21)$$

$$g_{NL} \simeq 13.4 \frac{M_p^4}{f^4} \frac{\Gamma_\sigma}{m} \theta_*^{-2}. \quad (3.22)$$

Therefore, the coefficient c is roughly given by

$$c \simeq 1.34 \frac{M_p^2}{f^2} \sqrt{\frac{\Gamma_\sigma}{m}}. \quad (3.23)$$

Using $f/M_p = 5 \times 10^{-3}$ and $\Gamma_\sigma/m = 10^{-4}$, $c \simeq 536$ which is roughly the same as that for the axion-type curvaton model. A general discussion for the curvaton model with a small correction to the quadratic potential is given in the Appendix.

3.2 Mixed scenario

In the previous subsection, where we assumed that the total primordial power spectrum is generated by the curvaton only, we saw that, having fixed $f/M_p = 5 \times 10^{-3}$, the value of $\Gamma_\sigma/m = 10^{-4}$ is too large for r to satisfy observational constraints. We know from Eq. (2.15) that r scales linearly with Γ_σ/m for the quadratic case. From Fig. 3 it seems that for the axion-type case also r scales linearly with Γ_σ/m , though it is not obvious from the equations. Hence, this value was enough to demonstrate the physics.

In this subsection we consider the scenario where the final curvature perturbations are contributed by both inflaton and curvaton fluctuations. This scenario has been invoked in [8] to naturally achieve a red-tilted primordial power spectrum in the curvaton model. It is convenient to introduce a new parameter β ,

$$\beta = P_{\zeta_\sigma}/P_\zeta, \quad (3.24)$$

where P_ζ is the total primordial power spectrum including the contribution from inflaton, and hence $\beta \in [0, 1]$. Then the effective non-Gaussianity parameters becomes

$$f_{NL}^{eff} = \beta^2 f_{NL}, \quad g_{NL}^{eff} = \beta^3 g_{NL}. \quad (3.25)$$

See [8, 11] for detail. The same result of f_{NL}^{eff} in the mixed scenario is also obtained in [13]. If $g_{NL} = cf_{NL}$,

$$g_{NL}^{eff} = \beta cf_{NL}^{eff} \quad (3.26)$$

where g_{NL}^{eff} is suppressed by a small factor β with respect to f_{NL}^{eff} . In [11], the author found

$$g_{NL} = cf_{NL}^2 \quad (3.27)$$

for the curvaton model in which the curvaton has a polynomial potential and the quadratic term is subdominant during inflation. In this case,

$$g_{NL}^{eff} = \frac{c}{\beta} (f_{NL}^{eff})^2, \quad (3.28)$$

which is enhanced by a factor $1/\beta$. A large g_{NL} is expected in the curvaton model. In general, $\tau_{NL}^{eff} \geq \frac{36}{25} (f_{NL}^{eff})^2$ in the multi-field case [19]. In particular, in the mixed scenario, τ_{NL}^{eff} is enhanced by a factor $1/\beta$, namely

$$\tau_{NL}^{eff} = \frac{36}{25\beta} (f_{NL}^{eff})^2. \quad (3.29)$$

For the axion-type curvaton model β can be expressed as

$$\beta \equiv \frac{P_{\zeta_\sigma}}{P_\zeta} = \frac{r}{8} N_*^2 \frac{M_p^2}{f^2}. \quad (3.30)$$

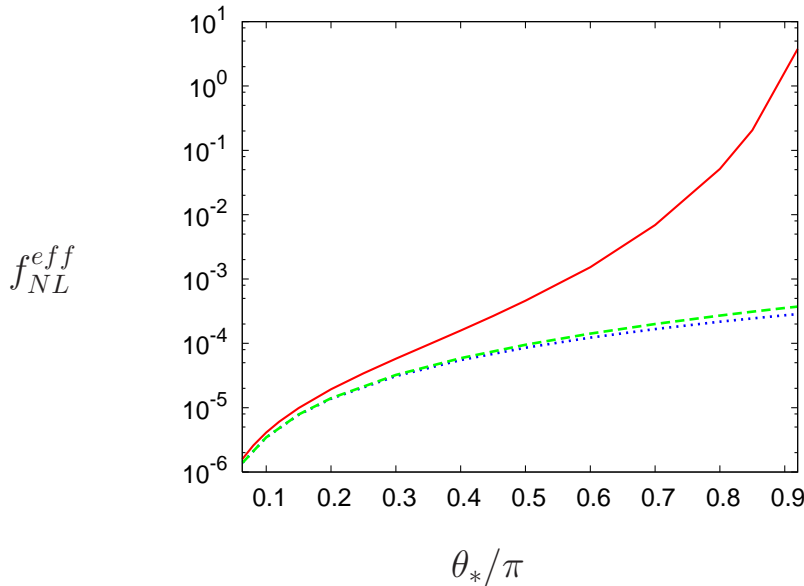


Figure 7: Plot of f_{NL}^{eff} . The red (solid), blue (dotted) and green (dashed) lines correspond to axion-type, quadratic and quadratic with σ^4 correction models, respectively.

If $r < 8f^2/(N_*'^2 M_p^2)$, then $\beta < 1$, which implies that the quantum fluctuation of the curvaton only contributes a part of the total primordial curvature perturbation. In Figs. 7, 8 and 9, we have plotted f_{NL}^{eff} , g_{NL}^{eff} and τ_{NL}^{eff} , respectively. The parameter values we have used for these plots are $f/M_p = 5 \times 10^{-3}$, $\Gamma_\sigma/m = 10^{-4}$ and $r = 0.1$. We see that the values are suppressed by factor of β^2 for f_{NL} and by β^3 for g_{NL} and τ_{NL} .

4 Conclusion

The curvaton model is one of the few models for the generation of primordial density perturbations which predict large non-Gaussianity and is potentially testable in the near future in upcoming experiments such as Planck. Specific models that have been well studied and for which analytic approximate results can be obtained are the simplest ones such as a polynomial potential [11]. In this paper we solved the evolution equations for the quadratic potential to see whether the analytic approximations are really accurate. We found that the analytic expression underestimates the exact answer by about factor of two. The reason is that the axion does not exactly behave as dust-like matter when it oscillates about the minimum of its potential. The friction term in the axion equation of motion, though small, is not negligible and makes the energy density decrease with respect to the scale factor as $a^{-3+\epsilon}$, where ϵ is small and positive.

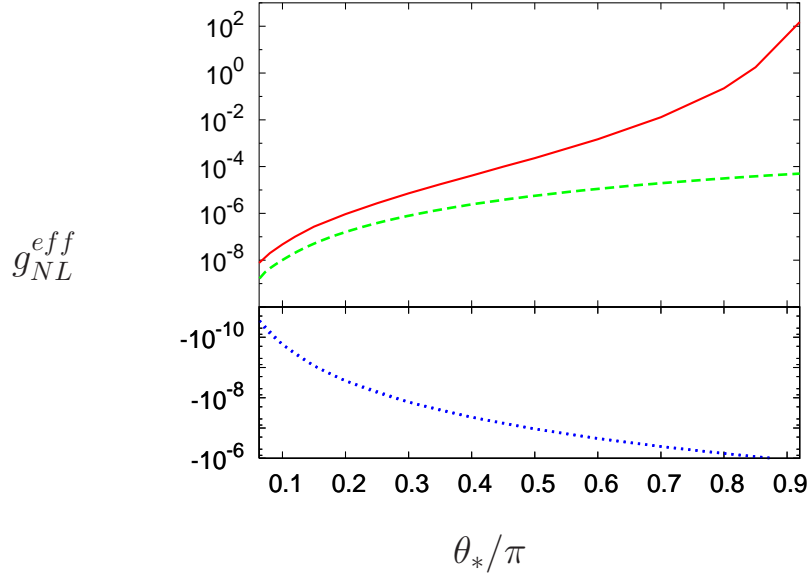


Figure 8: Plot of g_{NL}^{eff} . The red (solid), blue (dotted) and green (dashed) lines correspond to axion-type, quadratic and quadratic with σ^4 correction models, respectively.

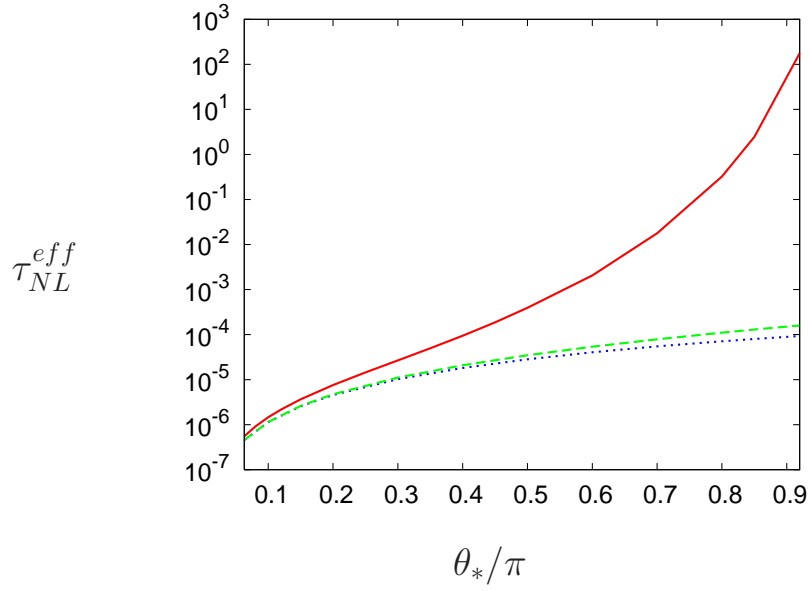


Figure 9: Plot of τ_{NL}^{eff} . The red (solid), blue (dotted) and green (dashed) lines correspond to axion-type, quadratic and quadratic with σ^4 correction models, respectively.

Our main motivation in this paper was to understand the non-linearity parameter g_{NL} in the axion-type curvaton model. To achieve this goal we used the δN formalism to solve for the two non-linearity parameters. The axion type model is very hard to solve analytically for large field values. In addition, computing g_{NL} numerically is much harder than f_{NL} since it contains a third order derivative as against the second order derivative of f_{NL} . We have evaluated the tensor-scalar ratio r using WMAP normalization and used it to compute f_{NL} and g_{NL} . We compare them with results for the curvaton with quadratic potential. We found that r is much smaller for the axion-type case compared to the quadratic potential when $\sigma_* \sim f$. The difference between them becomes increasingly more pronounced at larger field values. g_{NL} is found to be positive, unlike the quadratic case where it is negative, and the amplitude of g_{NL} is much larger. We also found that there is a nearly linear scaling between g_{NL} and f_{NL} , with small deviation from linearity at large field values. Lastly, we considered a mixed scenario where both the inflaton and the curvaton contribute to the primordial power spectrum. We have found that g_{NL} and f_{NL} are greatly suppressed with respect to the case where only the curvaton contributes. Moreover, g_{NL}^{eff} is suppressed with respect to f_{NL}^{eff} , whereas, τ_{NL}^{eff} is enhanced and hence it would be inconsistent to ignore the contribution to the overall primordial non-Gaussianity from τ_{NL}^{eff} .

We conclude with a few remarks on the trispectrum. Usually the trispectrum is characterized by two parameters τ_{NL} and g_{NL} . While f_{NL} is well studied for a variety of curvaton models in the literature, the trispectrum is not as well studied. One reason is the technical difficulty of having to deal with third order perturbations. Several recent works have shown that τ_{NL} and g_{NL} can be as important as, if not more than, f_{NL} . On the observation side much work has been devoted to constraining the value of f_{NL} using the CMB observations. It makes sense to ignore τ_{NL} and g_{NL} if their contribution is small. However, we need to take them into account if the trispectrum is large since they are independent parameters and have the potential to discriminate between different curvaton models. It would be very interesting to study the implications of large τ_{NL} and g_{NL} on the CMBR and we are working along those lines.

Acknowledgments

We would like to acknowledge use of QUEST, one of the computing facilities at Korea Institute for Advanced Study, where the numerical computation in this paper was carried out. QGH would like to thank K. Nakayama for useful discussions. We would also like to thank C. Byrnes for commenting on the first version of this paper and pointing out the relevance of τ_{NL} .

A g_{NL} vs. f_{NL} in the curvaton model with small deviation from quadratic potential

The non-Gaussianity for the curvaton model with small deviation from quadratic potential is investigated in [10]. In this appendix we extend the previous discussion. Assume the curvaton potential is given by

$$V(\sigma) = \frac{1}{2}m^2\sigma^2 + \lambda m^4 \left(\frac{\sigma}{m}\right)^n, \quad (\text{A.1})$$

where $n \geq 2$. If $n < 2$, the correction term becomes dominant around $\sigma = 0$. The correction in the equation of motion is small if $|s| \ll 1/n$, where

$$s = \lambda \left(\frac{\sigma_*}{m}\right)^{n-2}. \quad (\text{A.2})$$

The general result is given in [10]. Here $\lambda = -m^2/(24f^2)$ and $s = -\delta$ for the axion-type curvaton model. For case of the small correction, f_{NL} and g_{NL} take the form

$$f_{NL} \simeq \frac{5}{4f_D}, \quad (\text{A.3})$$

$$g_{NL} \simeq -\frac{25}{24}v(n)\frac{s}{f_D^2} - \frac{25}{6f_D} \quad (\text{A.4})$$

where

$$v(n) = -n^2(n-1)(n-2)2^{\frac{n-1}{4}}\Gamma(5/4)^{n-1}\pi \times \left[J_{\frac{1}{4}}\left(\frac{1}{2}\right) \int_0^{\frac{1}{2}} J_{\frac{1}{4}}^{n-1}(x)Y_{\frac{1}{4}}(x)x^{\frac{6-n}{4}} dx - Y_{\frac{1}{4}}\left(\frac{1}{2}\right) \int_0^{\frac{1}{2}} J_{\frac{1}{4}}^n(x)x^{\frac{6-n}{4}} dx \right], \quad (\text{A.5})$$

which shows up in Fig. 10. From Eq.(A.4), g_{NL} becomes positive if

$$s < -\frac{4}{v(n)}f_D. \quad (\text{A.6})$$

If g_{NL} is dominated by the second term in Eq.(A.4), $g_{NL} \simeq -\frac{10}{3}f_{NL}$. Now we focus on the case of $|s| \gg 4f_D/v(n)$, namely

$$g_{NL} \simeq -\frac{25}{24}v(n)\frac{s}{f_D^2}. \quad (\text{A.7})$$

Using Eq.(2.14), we have

$$f_{NL} \simeq 10\frac{M_p^2}{m^2}\sqrt{\frac{\Gamma_\sigma}{m}}\left(\frac{\sigma_*}{m}\right)^{-2}, \quad (\text{A.8})$$

$$g_{NL} \simeq -\frac{200}{3}v(n)\lambda\frac{M_p^4}{m^4}\frac{\Gamma_\sigma}{m}\left(\frac{\sigma_*}{m}\right)^{n-6}. \quad (\text{A.9})$$

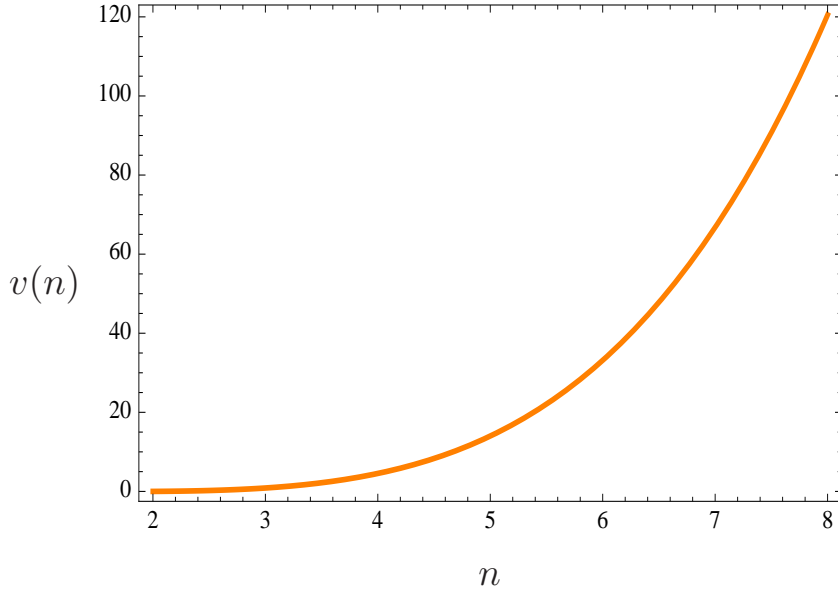


Figure 10: Plot of $v(n)$ as a function of n .

Therefore,

$$g_{NL} \simeq c f_{NL}^{3-n/2}, \quad (\text{A.10})$$

where

$$c = -\frac{200}{3} 10^{n/2-3} v(n) \lambda \left(\frac{M_p}{m} \right)^{n-2} \left(\frac{\Gamma_\sigma}{m} \right)^{\frac{n-2}{4}}. \quad (\text{A.11})$$

For $n = 2$, $c = v(n) = 0$ and g_{NL} still linearly depends on f_{NL} . In the mixed scenario,

$$g_{NL}^{eff} = \beta^{n-3} c (f_{NL}^{eff})^{3-n/2}. \quad (\text{A.12})$$

The second order non-Gaussianity parameter is enhanced in the mixed scenario if $n < 3$. However, for $2 \leq n < 3$, $v(n) \leq 1$, and hence a large absolute value of g_{NL} is quite unlikely.

References

- [1] A. H. Guth, “The Inflationary Universe: A Possible Solution To The Horizon And Flatness Problems,” *Phys. Rev. D* **23**, 347 (1981);
A. D. Linde, “A New Inflationary Universe Scenario: A Possible Solution Of The Horizon, Flatness, Homogeneity, Isotropy And Primordial Monopole Problems,” *Phys. Lett. B* **108**, 389 (1982);
A. Albrecht and P. J. Steinhardt, “Cosmology For Grand Unified Theories With Radiatively Induced Symmetry Breaking,” *Phys. Rev. Lett.* **48**, 1220 (1982).

- [2] A. D. Linde and V. F. Mukhanov, “Nongaussian isocurvature perturbations from inflation,” *Phys. Rev. D* **56**, 535 (1997) [arXiv:astro-ph/9610219];
 K. Enqvist and M. S. Sloth, “Adiabatic CMB perturbations in pre big bang string cosmology,” *Nucl. Phys. B* **626**, 395 (2002) [arXiv:hep-ph/0109214];
 D. H. Lyth and D. Wands, “Generating the curvature perturbation without an inflaton,” *Phys. Lett. B* **524**, 5 (2002) [arXiv:hep-ph/0110002];
 T. Moroi and T. Takahashi, “Effects of cosmological moduli fields on cosmic microwave background,” *Phys. Lett. B* **522**, 215 (2001) [Erratum-ibid. B **539**, 303 (2002)] [arXiv:hep-ph/0110096].
- [3] N. Bartolo, E. Komatsu, S. Matarrese and A. Riotto, “Non-Gaussianity from inflation: Theory and observations,” *Phys. Rept.* **402**, 103 (2004) [arXiv:astro-ph/0406398];
 L. Alabidi and D. H. Lyth, “Inflation models and observation,” *JCAP* **0605**, 016 (2006) [arXiv:astro-ph/0510441];
 C. T. Byrnes, M. Sasaki and D. Wands, “The primordial trispectrum from inflation,” *Phys. Rev. D* **74**, 123519 (2006) [arXiv:astro-ph/0611075].
- [4] J. M. Maldacena, “Non-Gaussian features of primordial fluctuations in single field inflationary models,” *JHEP* **0305**, 013 (2003) [arXiv:astro-ph/0210603].
- [5] E. Komatsu *et al.* [WMAP Collaboration], “Five-Year Wilkinson Microwave Anisotropy Probe (WMAP) Observations:Cosmological Interpretation,” arXiv:0803.0547 [astro-ph].
- [6] K. M. Smith, L. Senatore and M. Zaldarriaga, arXiv:0901.2572 [astro-ph].
- [7] Q. G. Huang, “Large Non-Gaussianity Implication for Curvaton Scenario,” *Phys. Lett. B* **669**, 260 (2008) [arXiv:0801.0467 [hep-th]];
 T. Matsuda, “Modulated Inflation,” *Phys. Lett. B* **665**, 338 (2008) [arXiv:0801.2648 [hep-ph]];
 K. Ichikawa, T. Suyama, T. Takahashi and M. Yamaguchi, “Non-Gaussianity, Spectral Index and Tensor Modes in Mixed Inflaton and Curvaton Models,” *Phys. Rev. D* **78**, 023513 (2008) [arXiv:0802.4138 [astro-ph]];
 T. Suyama and F. Takahashi, “Non-Gaussianity from Symmetry,” *JCAP* **0809**, 007 (2008) [arXiv:0804.0425 [astro-ph]];
 X. Gao, “Primordial Non-Gaussianities of General Multiple Field Inflation,” *JCAP* **0806**, 029 (2008) [arXiv:0804.1055 [astro-ph]];
 M. Beltran, “Isocurvature, non-gaussianity and the curvaton model,” *Phys. Rev. D* **78**, 023530 (2008) [arXiv:0804.1097 [astro-ph]];
 B. Chen, Y. Wang and W. Xue, “Inflationary NonGaussianity from Thermal Fluctuations,” *JCAP* **0805**, 014 (2008) [arXiv:0712.2345 [hep-th]];
 M. Li, T. Wang and Y. Wang, “General Single Field Inflation with Large Positive

Non-Gaussianity,” JCAP **0803**, 028 (2008) [arXiv:0801.0040 [astro-ph]];

M. Li, C. Lin, T. Wang and Y. Wang, “Non-Gaussianity, Isocurvature Perturbation, Gravitational Waves and a No-Go Theorem for Isocurvaton,” arXiv:0805.1299 [astro-ph];

M. Sasaki, “Multi-brid inflation and non-Gaussianity,” Prog. Theor. Phys. **120**, 159 (2008) [arXiv:0805.0974 [astro-ph]];

S. Li, Y. F. Cai and Y. S. Piao, “DBI-Curvaton,” arXiv:0806.2363 [hep-ph];

Q. G. Huang, “Spectral Index in Curvaton Scenario,” Phys. Rev. D **78**, 043515 (2008) [arXiv:0807.0050 [hep-th]];

M. Sasaki, “Multi-brid inflation and non-Gaussianity,” Prog. Theor. Phys. **120**, 159 (2008) [arXiv:0805.0974 [astro-ph]];

M. Li and Y. Wang, “Consistency Relations for Non-Gaussianity,” JCAP **0809**, 018 (2008) [arXiv:0807.3058 [hep-th]];

M. Li and C. Lin, “Reconstruction of the isocurvaton scenario,” arXiv:0807.4352 [astro-ph];

M. Kawasaki, K. Nakayama, T. Sekiguchi, T. Suyama and F. Takahashi, “Non-Gaussianity from isocurvature perturbations,” JCAP **0811**, 019 (2008) [arXiv:0808.0009 [astro-ph]];

M. Kawasaki, K. Nakayama and F. Takahashi, “Non-Gaussianity from Baryon Asymmetry,” JCAP **0901**, 002 (2009) [arXiv:0809.2242 [hep-ph]];

K. Dimopoulos, D. H. Lyth and Y. Rodriguez, “Statistical anisotropy of the curvature perturbation from vector field perturbations,” arXiv:0809.1055 [astro-ph];

T. Moroi and T. Takahashi, “Non-Gaussianity and Baryonic Isocurvature Fluctuations in the Curvaton Scenario,” arXiv:0810.0189 [hep-ph];

M. Kawasaki, K. Nakayama, T. Sekiguchi, T. Suyama and F. Takahashi, “A General Analysis of Non-Gaussianity from Isocurvature Perturbations,” arXiv:0810.0208 [astro-ph];

T. Matsuda, “Non-standard kinetic term as a natural source of non-Gaussianity,” JHEP **0810**, 089 (2008) [arXiv:0810.3291 [hep-ph]];

C. T. Byrnes, K. Y. Choi and L. M. H. Hall, “Large non-Gaussianity from two-component hybrid inflation,” arXiv:0812.0807 [astro-ph];

C. Hikage, K. Koyama, T. Matsubara, T. Takahashi and M. Yamaguchi, “Limits on Isocurvature Perturbations from Non-Gaussianity in WMAP Temperature Anisotropy,” arXiv:0812.3500 [astro-ph];

P. D. Meerburg, J. P. van der Schaar and P. S. Corasaniti, “Signatures of Initial State Modifications on Bispectrum Statistics,” arXiv:0901.4044 [hep-th];

H. R. S. Cogollo, Y. Rodriguez and C. A. Valenzuela-Toledo, “On the Issue of the ζ Series Convergence and Loop Corrections in the Generation of Observable Primordial Non-Gaussianity in Slow-Roll Inflation. Part I: the Bispectrum,” JCAP **0808**, 029 (2008) [arXiv:0806.1546 [astro-ph]];

- Y. Rodriguez and C. A. Valenzuela-Toledo, “On the Issue of the ζ Series Convergence and Loop Corrections in the Generation of Observable Primordial Non-Gaussianity in Slow-Roll Inflation. Part II: the Trispectrum,” arXiv:0811.4092 [astro-ph].
- [8] Q. G. Huang, “The N-vaton,” JCAP **0809**, 017 (2008) [arXiv:0807.1567 [hep-th]].
- [9] K. Enqvist and T. Takahashi, “Signatures of Non-Gaussianity in the Curvaton Model,” JCAP **0809**, 012 (2008) [arXiv:0807.3069 [astro-ph]].
- [10] Q. G. Huang and Y. Wang, “Curvaton Dynamics and the Non-Linearity Parameters in Curvaton Model,” JCAP **0809**, 025 (2008) [arXiv:0808.1168 [hep-th]].
- [11] Q. G. Huang, “Curvaton with Polynomial Potential,” JCAP **0811**, 005 (2008) [arXiv:0808.1793 [hep-th]].
- [12] M. Kawasaki, K. Nakayama and F. Takahashi, “Hilltop Non-Gaussianity,” arXiv:0810.1585 [hep-ph].
- [13] D. Langlois, F. Vernizzi and D. Wands, “Non-linear isocurvature perturbations and non-Gaussianities,” JCAP **0812**, 004 (2008) [arXiv:0809.4646 [astro-ph]].
- [14] K. Dimopoulos, D. H. Lyth, A. Notari and A. Riotto, “The curvaton as a Pseudo-Nambu-Goldstone boson,” JHEP **0307**, 053 (2003) [arXiv:hep-ph/0304050];
E. J. Chun, K. Dimopoulos and D. Lyth, “Curvaton and QCD axion in supersymmetric theories,” Phys. Rev. D **70**, 103510 (2004) [arXiv:hep-ph/0402059].
- [15] P. Svrcek and E. Witten, “Axions in string theory,” JHEP **0606**, 051 (2006) [arXiv:hep-th/0605206].
- [16] A. A. Starobinsky, “Multicomponent de Sitter (Inflationary) Stages and the Generation of Perturbations,” JETP Lett. **42** (1985) 152;
M. Sasaki and E. D. Stewart, “A General Analytic Formula For The Spectral Index Of The Density Perturbations Produced During Inflation,” Prog. Theor. Phys. **95**, 71 (1996) [arXiv:astro-ph/9507001];
M. Sasaki and T. Tanaka, “Super-horizon scale dynamics of multi-scalar inflation,” Prog. Theor. Phys. **99**, 763 (1998) [arXiv:gr-qc/9801017];
D. H. Lyth, K. A. Malik and M. Sasaki, “A general proof of the conservation of the curvature perturbation,” JCAP **0505**, 004 (2005) [arXiv:astro-ph/0411220];
D. H. Lyth and Y. Rodriguez, “The inflationary prediction for primordial non-gaussianity,” Phys. Rev. Lett. **95**, 121302 (2005) [arXiv:astro-ph/0504045].
- [17] M. Sasaki, J. Valiviita and D. Wands, “Non-gaussianity of the primordial perturbation in the curvaton model,” Phys. Rev. D **74**, 103003 (2006) [arXiv:astro-ph/0607627].

- [18] T. S. Bunch and P. C. W. Davies, “Quantum Field Theory In De Sitter Space: Renormalization By Point Splitting,” *Proc. Roy. Soc. Lond. A* **360** (1978) 117;
A. Vilenkin and L. H. Ford, “Gravitational Effects Upon Cosmological Phase Transitions,” *Phys. Rev. D* **26**, 1231 (1982);
A. D. Linde, “Scalar Field Fluctuations In Expanding Universe And The New Inflationary Universe Scenario,” *Phys. Lett. B* **116**, 335 (1982);
A. A. Starobinsky and J. Yokoyama, “Equilibrium state of a selfinteracting scalar field in the De Sitter background,” *Phys. Rev. D* **50**, 6357 (1994) [arXiv:astro-ph/9407016].
- [19] T. Suyama and M. Yamaguchi, “Non-Gaussianity in the modulated reheating scenario,” *Phys. Rev. D* **77**, 023505 (2008) [arXiv:0709.2545 [astro-ph]].